

## Segmentation of Cerebral Vasculature

### Introduction

Cerebrovascular disease (stroke) is among the leading causes of death in western industrial nations, besides cardiac and cancer-related deaths. A stroke may be caused by a blockage of blood vessels due to a blood clot (ischemic) or a rupture of blood vessels or aneurysms (hemorrhagic). Regarding the diagnosis and treatment of cerebral aneurysms, 3-D digital subtraction angiography (DSA) image data delivers indispensable information to analyze the aneurysm geometry and its location to come up with a clinical decision. While the causes for the appearance of aneurysms are not entirely understood, it is assumed that hemodynamic forces are an important contributing factor. Especially the position and orientation of the aneurysm neck area seems to play an important role for the blood flow pattern within aneurysms. For further studies like blood flow simulations, the segmentation of aneurysms together with parent arteries is an important prerequisite.

Simple segmentation techniques like intensity thresholding or region growing only consider voxel-based gray-value information and thus may lead to leakages or holes within the segmentation volume due to noisy 3-D DSA image data. Therefore, an approach based on curve evolution theory and the level set [4] framework is applied. Edge based geodesic active contours [2] (GAC) are extended by a vessel shape regularizer to reduce these afore-mentioned drawbacks. Moreover, by incorporating knowledge about the appearance of a healthy vessel, the proposed method is able to omit pathologic structures like aneurysms from the segmentation, which is necessary for blood flow simulations.

The application of GAC level sets for vessel segmentation has the advantage to naturally handle topological changes like vessel bifurcations due to its implicit contour description.

The objective of this paper is to segment a cerebral vessel tree omitting areas with vascular disease e.g. aneurysms. Our segmentation method was experimentally evaluated on ten different patient data sets against a gold standard segmentation in terms of sensitivity, average surface distance and Hausdorff distance.

### Methods

The chosen segmentation method is based on the geodesic active contours (GAC) approach [2]. An initial curve is iteratively deformed, until it coincides with the object borders to be segmented.

The evolving surface is implicitly represented by embedding it as the zero level set of a level set function  $\phi$ . This allows handling topological changes intrinsically. Moreover, no re-parameterization of the evolving

surface is required for vessel bifurcations due to the implicit representation.

The function  $\phi$  maps time dependent points  $(\mathbf{x}, t)$  within the image domain  $\Omega$  to scalar values. It is a parameter-free mapping, because  $\Gamma$  typically denotes the location of the points for which the values are zero - the zero level set. This zero level set splits the image in two regions, where negative values are assumed to be inside and positive values are assumed to be outside the contour (or vice versa). The absolute value at a certain point  $\mathbf{x}$  is respectively defined as a distance from the zero level set. The deformation of the surface is governed by a speed function which guides the surface into the desired directions, e.g. fast movement in homogeneous regions and slow movement while approaching edges. In this case, an edge refers to the boundary between vessel and non-vessel structures.

Since cerebral arteries can be considered as tubular structures, our speed function not only consists of edge-based features and a standard curvature dependent smoothness term, but also of a vessel shape regularizer. Hence, it penalizes deformations of the surface which deviate from the appearance of regular tubular vasculature. The entire level set function  $\phi$  consists of the following terms:

$$\frac{\partial \phi}{\partial t} = -\alpha A(\mathbf{x})\nabla \phi - \beta P(\mathbf{x})|\nabla \phi| + \gamma Z(\mathbf{x})\kappa|\nabla \phi| + \delta T(\mathbf{x}) \quad (1)$$

where  $A(\mathbf{x})$  denotes the advection vector field,  $P(\mathbf{x})$  is the propagation term,  $Z(\mathbf{x})$  is the spatial modifier term for the curvature  $\kappa$  and  $T(\mathbf{x})$  represents the additional vessel shape regularizer, which was originally introduced by Nain [3].  $\alpha$ ,  $\beta$ ,  $\gamma$ , and  $\delta$  denote weighting factors for the individual terms. We refer to [5] for more details concerning the advection, propagation and spatial term.

The shape regularizer  $T(\mathbf{x})$  is a region-based measurement, which quantifies the similarity of the local surface geometry to a tubular structure. This region  $\mathbf{R}$ , representing the entire vessel tree with an aneurysm and some noise, is obtained by a seeded region growing approach. Fig. 1 illustrates the region  $\mathbf{R}$  based on a phantom vessel structure. In the following, all points inside and on the contour of  $\mathbf{R}$  will be considered. A local region-based neighborhood description  $B(\mathbf{x}, r)$  is defined to determine widening and

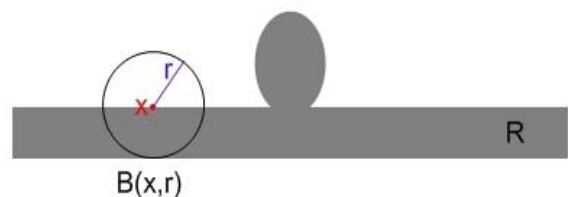


**Fig. 1** Phantom image of a 2D vessel with an aneurysm.  $\mathbf{R}$  denotes the region used by the vessel regularizer and  $B(\mathbf{x}, r)$  the neighborhood to compute the vessel shape measurement  $\epsilon_l$ .

potential leakages. For every point within the region  $R$ , a local neighborhood  $B(x, r)$  (in 2D it's a circle and in 3D it becomes a sphere) with a certain radius is considered to compute a measurement  $\varepsilon_1$ , which denotes the percentage of points lying within the region  $R$  and within the neighborhood  $B(x, r)$ :

$$\varepsilon_1(\mathbf{x}) = \int_{B(\mathbf{x}, r)} X(\mathbf{y}) d\mathbf{y} \text{ where } X(\mathbf{y}) = \begin{cases} 1 & \text{if } \mathbf{y} \in R \\ 0 & \text{if } \mathbf{y} \notin R \end{cases} \quad (2)$$

Given a certain ball radius  $r$ , points at widening regions result in higher values for  $\varepsilon_1$  than those inside the vessel structure. The maximum ball radius must be specified by the user and should represent the largest vessel radius in the image data.

The final shape vessel term  $T(\mathbf{x})$  is again based on  $\varepsilon_1$ :

$$T(\mathbf{x}) := \varepsilon_2(\mathbf{x}, p)$$

$$\varepsilon_2(\mathbf{x}, p) = \varepsilon_1^p(\mathbf{x}) + p \int_{B(\mathbf{x}, r)} \varepsilon_1^{p-1}(\mathbf{y}) X(\mathbf{y}) d\mathbf{y} \quad (3)$$

So each point is quantified in terms of tubular shape by its  $\varepsilon_1$  measure plus the sum of all  $\varepsilon_1$  values within the neighborhood  $B(x, r)$ . For example, points being near the aneurysm neck area get higher values since their neighboring points lie in a widening area and thus contribute high  $\varepsilon_1$  measurement values to the considered area  $B(x, r)$ . This can be seen in Fig. 2.

Our proposed segmentation approach starts with a region growing segmentation delivering the initialization for the subsequent level set evolution. This segmentation contains the aneurysm and maybe some leakages. The performance of our extended level set method pulls the segmentation out of areas describing abnormal vessel structures and widening like aneurysms or leakages.

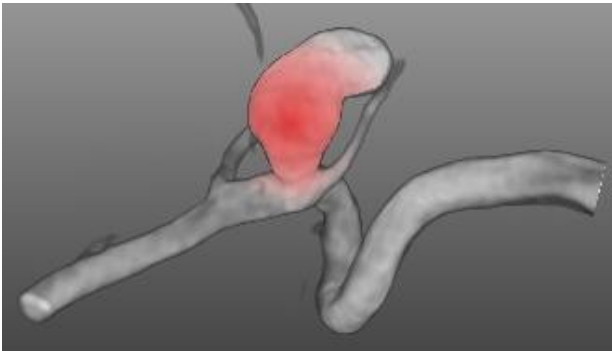


**Fig. 2** Overlay of cerebral vessel tree with its corresponding  $\varepsilon_2$  measurement values. The red color indicates a widening area (aneurysm neck) and thus large  $\varepsilon_2$  measurement values.

## Results

The evaluation of our proposed method was done on ten different 3D DSA patient data sets acquired from a

Siemens AXIOM Artis dBA TWIN x-ray fluoroscopy system during clinical interventions. The image sizes vary between  $256 \times 256 \times 200$  and the voxel spacing in  $x/y/z$  direction is  $0.2/0.2/0.2$  mm. A gold standard segmentation without the aneurysm dome region was obtained for each data set using ITK-SNAP ([www.itksnap.org](http://www.itksnap.org)).

The segmentation results were evaluated according to sensitivity, average surface distance (AVD) and the Hausdorff distance (HD) measuring the deviations to the gold standard segmentation. A detailed overview about the segmentation results is given by table 1. The proposed segmentation approach reaches a sensitivity value of more than 90% for five patient data sets. The Hausdorff distance ranges between 4.6 and 16.9 mm. Larger values are caused by the fact that a small bleb of the aneurysm region remain (see Fig. 3) even after the segmentation is done. The AVD was applied to reduce the influence of those blebs on the evaluation of the segmentation result. Fig. 3 gives a visual impression of the segmentation result based on the  $\varepsilon_2$  measurement values illustrated in Fig. 2.

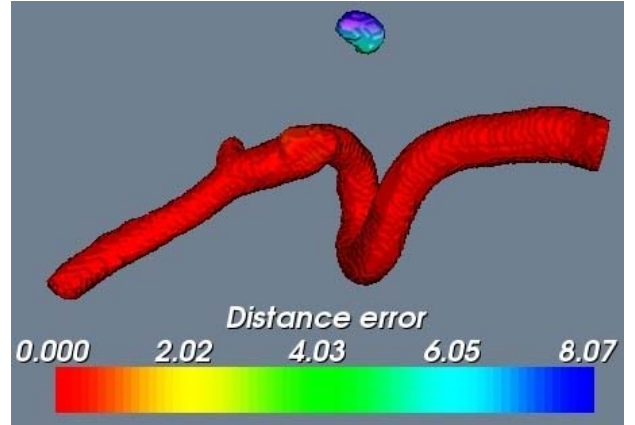


**Fig. 3** Final segmentation result quantified according to the Hausdorff distance (distance error in mm) to the corresponding gold standard segmentation.

Dataset	Sensitivity	AVD	HD
P. 1	0.99481	0.1403	12.927
P. 2	0.94996	0.3617	5.6185
P. 3	0.60567	0.7741	7.6710
P. 4	0.53699	1.2694	10.095
P. 5	0.71302	0.4087	13.507
P. 6	0.9999	0.3375	10.219
P. 7	0.92808	0.1502	4.5645
P. 8	0.8135	0.5642	16.870
P. 9	0.32135	2.2738	14.911
P. 10	0.98667	0.1760	8.067

Table 1 Quantitative segmentation results given by sensitivity, specificity, average surface distance (AVD in mm) and Hausdorff distance (HD in mm).

## Discussion and Conclusion

This paper describes a vessel segmentation approach based on level set active contours extended by a vessel shape regularizer originally introduced by Nain [3].

The speed function, evolving the initial contour, is enhanced by an additional term incorporating prior knowledge about vessels and penalizes the segmentation of non-tubular structures. The presented results show that a tubular constrained level set segmentation technique can be employed for cerebral vessel extraction without segmenting vascular disease like aneurysms. This enables the analysis the aneurysm neck area regarding its influence within CFD-based blood flow simulations in more details.

Future work involves the elimination of two drawbacks. Firstly, the segmentation is very sensitive to the user provided maximum vessel radius. If the diameter of the aneurysm neck and the thickest vessel structure are in a similar range, then the aneurysm would also become part of the segmentation. On the other hand, a small radius would ensure that the aneurysm is omitted in the segmentation, but thicker vessel structures easily will be discarded, too.

Secondly, the handling of the aneurysm neck area is challenging because the presented shape regularizer does not distinguish between widening areas caused by noise or due to an aneurysm. But the widening region at an aneurysm neck is just the area leading into the aneurysm dome and not the parent vessel part of the aneurysm itself.

Thus, an improved shape term should only penalize the entry area into the aneurysm dome and not the part of the vessel to which the aneurysm belongs to

Martenstr. 3  
Erlangen, 91058  
Germany  
yesim.alicioglu@googlemail.com

## Literature

- [1] Adams R., Bishop L. Seeded region growing. *IEEE Transactions on Pattern Recognition and Machine Intelligence*, Vol. 16(6):641-647, 1994
- [2] Caselles V., Kimmel R., Sapiro G. Geodesic active contours. *International Journal of Computer Vision*, Vol. 22(1):61-79, 1997.
- [3] Nain D., Yezzi A., Turk G. Vessel segmentation using a shape driven flow. In *Medical Image Computing and Computer-assisted Intervention - MICCAI*, pages 51-59, 2004.
- [4] Sethian J.A. Level Set Methods and Fast Marching Methods: Evolving Interfaces in Computational Geometry, Fluid Mechanics, Computer Vision, and Materials Science. *Cambridge University Press*, Second Edition, New York, 1999.
- [5] Ibanez L., Schroeder W. Ng L., Cates J. The ITK Software Guide, <http://www.itk.org>, November, 2005
- [6] Yushkevich P.A., Piven J., Hazlett H.C., Smith R.G., Ho S., Gee J. C., Gerig G. User-guided 3D active contour segmentation of anatomical structures: Significantly improved efficiency and reliability. *Neuroimage*, Vol. 31(3):1116-28, 2006

## Affiliation of the first Author

Yesim Alicioglu  
Chair of Pattern Recognition, University of Erlangen-Nuremberg